6
105. Jahrgang
Juni 2010
ISSN 0005-9900
A 1740

Beton- und Stahlbetonbau

Experimental and numeric examination of the load bearing behaviour of reinforced concrete slabs fitted with Cobiax cage modules

Ernst & Sohn
A Wiley Company

Reprint

Marcin Abramski
Andrej Albert
Karsten Pfeffer
Jürgen Schnell

Experimental and Numerical Investigations of the Load-Bearing Behaviour of Reinforced Concrete Slabs Using Spherical Void Formers

Solid flat slabs often prove to be the superior system in structural and industrial engineering applications. However, the high dead weights of the slabs can restrict their fields of application. Integrating void formers in the neutral zone provides a useful remedy, because of the noticeable weight reduction involved. In addition to reducing the dead load, the use of reinforcement steel and cement, which represent valuable resources from an ecological perspective, are also considerably reduced. The voids primarily impact the shear resistance of the slabs. Four test series' carried out using spherical "Cobiax" void former slabs are described in this paper. A reduction factor for describing the shear load bearing behaviour was identified from the test results and then integrated in the recently issued technical approval for the slab system. Test post analysis using the finite element method displayed good correlation between numerical investigations and experiment, such that future parameter studies based on these results in the course of development will prove highly valuable as a supplement to tests.

Fig. 1. Installed Cobiax Eco-Line system void formers before installing the upper reinforcement layer and concreting (erection of an office building in Bremen)

1 Introduction

Non-prestressed, solid, reinforced concrete slabs meet numerous requirements in structural and industrial engineering applications in terms of load bearing capacity, limiting deformations, acoustic and fire protection. They can be economically manufactured and therefore represent the normal mode of construction. However, the relatively large dead weight of the concrete often proves disadvantageous. This is especially the case for multi-storey buildings or buildings with difficult foundation situations, and for large slab spans in particular. Replacing the concrete by voids in those areas where it is not required from a structural perspective therefore represents an interesting optimisation option (Figure 1). The reduced dead weight not only means a lower rebar requirement in the slab, together with smaller deformations, but also lower overall building loads, making it possible to design using pillars and foundations with smaller dimensions. This in turn brings an additional ecological benefit, primarily because less reinforcement steel and cement are required. Some well-known projects where this technology has been used include the Zollverein school in Essen, Ozeaneum in Stralsund and the Elbphilharmonie in Hamburg.

If the spherical displacers are configured such that the minimum dimensions for the remaining webs and shear reinforcement no longer meet the minimum requirements to DIN 1045-1 [1] or EC 2, additional deliberations on the load bearing behaviour of the slabs are necessary. This paper reports on experimental investigations of slabs with integrated hollow void formers and their evaluations. The main focus of the investigations was to identify the shear resistance in the weakened cross-sections. The shear resistance in the critical punching areas was not investigated separately during the tests described here, because no void formers were planned for these zones.

2 Testing programme for determining shear resistance

This paper reports on the implementation and evaluation of four test series', carried out in 2007, 2008 and 2009 at the Technical Universities of Kaiserslautern and Darmstadt. Prior to this, slabs using hollow void formers had been comprehensively investigated in [2], [3] and [4].

All tests described in Sections 2 and 3 for identifying the shear resistance of the voided flat plate slabs without normal force were executed as four-point bending tests. The following parameters were varied:

- concrete quality (C12/15 ÷ C45/55),
- slab thickness (h = 30 cm ÷ 60 cm),
- shear slenderness (a/d = 2.7 ÷ 4.2),
- rebar percentage (ρ_l = 0.51 % and 0.75 %),
- sphere diameter (18; 31.5 cm und 45 cm).

The variable a used to calculate the shear slenderness mentioned above is regarded as the distance of the load transfer point to the support point; d is the effective structural depth.

2.1 Tests to determine the shear resistance on one-way spanning slabs without positioning cages

Six tests were carried out at the Technical University of Darmstadt on 30 and 60 cm thick slab strips [5]. The reinforcement steel positioning cages used in practical applications for buoyancy safety and void former fixation were not installed. This was done to avoid including their contribution to shear resistance in the test, because it is not incorporated in the design concept. The void formers were held in position by applying a surcharge to the upper layer of reinforcement during concreting. The dimensions in cross-section can be taken from Figure 2. The 18 and 45 cm diameter void formers were arranged in rows parallel to the span direction with a planned clear separation of 2 cm to 5 cm (Figure 2).

The mean cube compressive strength on the day of the test was between 18.0 and 51.0 N/mm^2. The net concrete cross-section perpendicular to the slab plane reduced by the void formers was 59% and 49% minimum respectively for the specimens with void former diameters 18 cm and 45 cm. The shear slenderness in the tests was a/d = 4.02 (h = 30 cm) and a/d = 4.23 (h = 60 cm). The degrees of bending reinforcement of 0.63 ÷ 0.75% were selected such that the planned shear failure would occur. Figure 3 shows a typical cracking pattern when the shear resistance is reached.

2.2 Tests to determine the shear resistance in zones of opposing moments

Slabs with axis-symmetrical void formers are particularly suited to use in multi-axially spanned flat roofs. Transversal bending, which may also act in opposing directions, occurs in the case of multi-axial spans, in addition to the main bending direction. Three additional tests were carried out at the TU Kaiserslautern to examine the shear re-

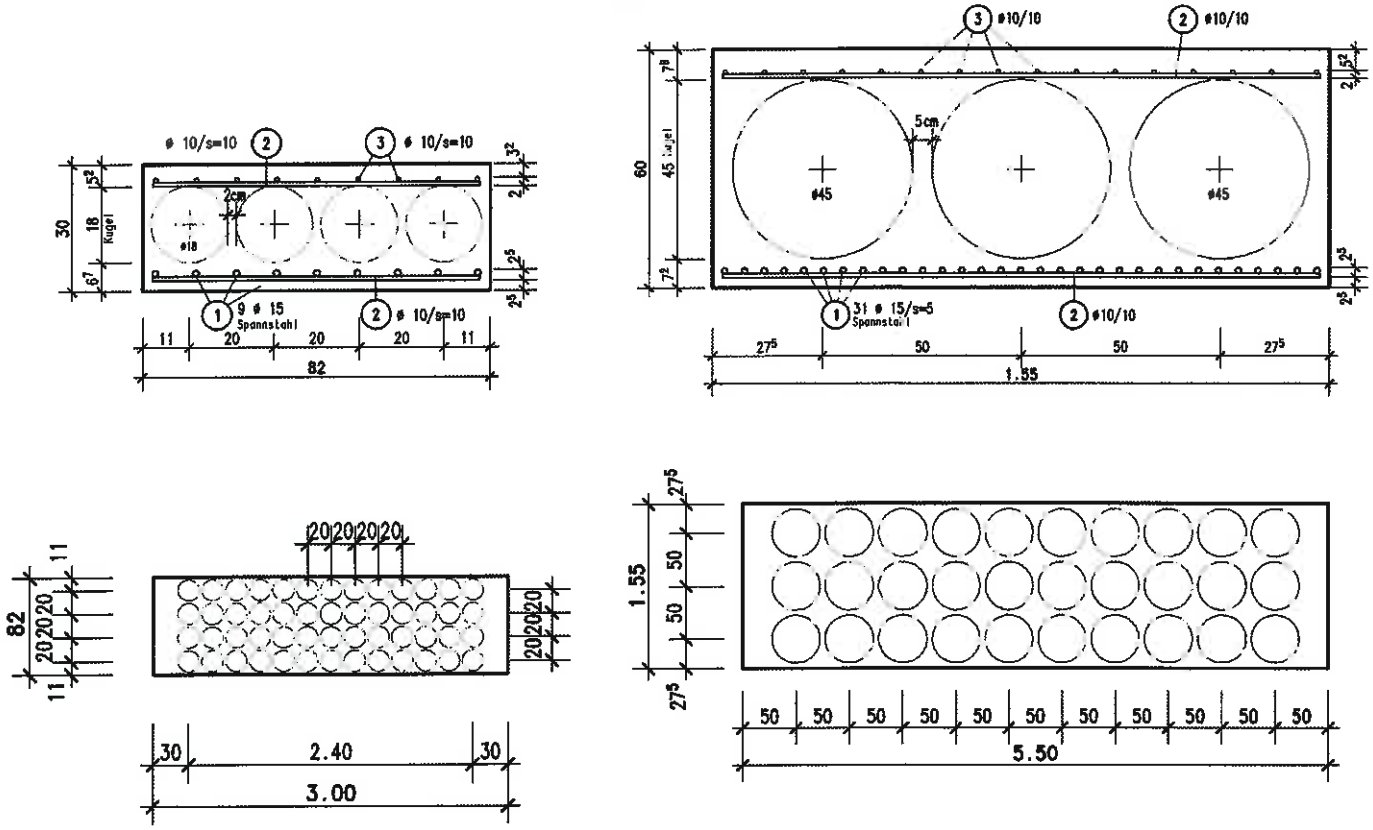

Fig. 2. The cross-sectional dimensions and void former configuration in the Darmstadt tests [5]

Fig. 3. Crack pattern after reaching shear force capacity in specimen V2Da of the Darmstadt tests [5]

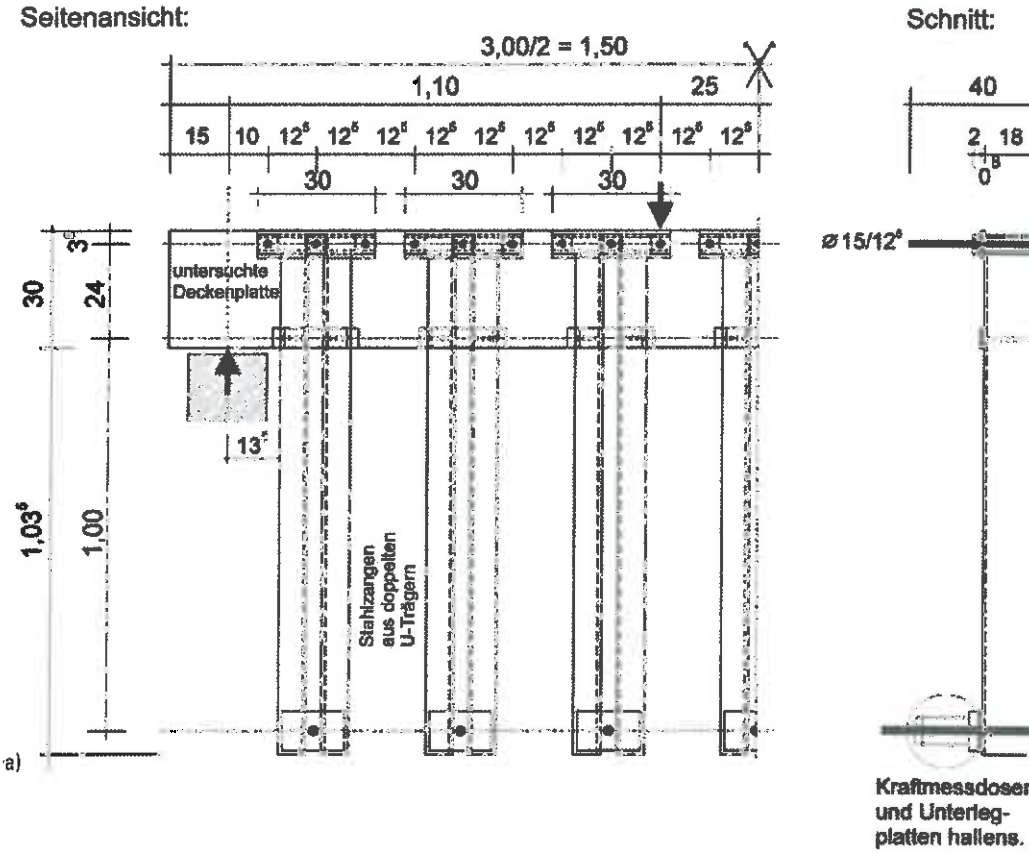

Fig. 4. The Kaiserslautern tests dedicated to shear force capacity in area of inversely acting bending moments: a) Steel tongs construction, b) Execution of a test

sistance in these slab areas. A loading device was designed by the Institut für Beton- und Fertigteilbau at Bochum University for this purpose. It allowed negative transverse bending moments to be transferred in four-point bending tests via a tong-like construction (Figure 4).

The transverse bending moments (tension on the upper slab face) were selected such that the design yield strength f_{yd} = 435 N/mm² was achieved in the upper transverse ϕ15/12.5 reinforcement. The tongs acted on the slab sides and moved smoothly with the aid of double Teflon discs. This generally prevented the tongs unintentionally acting as shear reinforcement.

All three investigated test specimens were manufactured using 30 cm thick in-situ concrete. The mean cube compressive strength on the day of the test was between 61.7 and 65.9 N/mm². The shear slenderness in the tests was a/d = 4.23.

The degree of bending reinforcement of 0.72% was also selected such that the planned shear failure would occur. Two test specimens (V1KL-2009 and V2KL-2009) were subjected to transversal bending during the actual test and one (V3KL-2009) was investigated without transversal bending. Two investigated test specimens (V1KL-2009 and V3KL-2009) were manufactured as solid slabs and one (V2KL-2009) as a void former slab. The void former diameter was 18 cm. The void formers were arranged diagonally in specimen V2KL-2009. The angles between the support axes and the rows of void formers was 22.5°

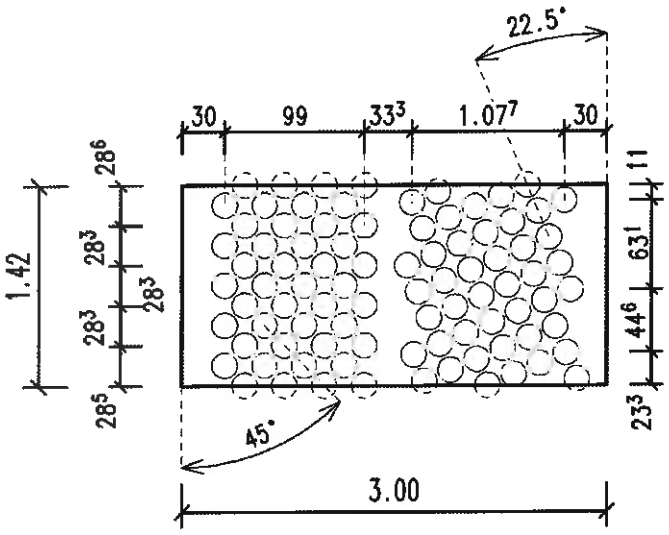

Fig. 5. Void former position in the specimen V2KL-2009

and 45° (Figure 5). This void former arrangement was selected to allow the most favourable case, without continuous concrete webs, to be examined. The positioning cages used in practice were not installed.

2.3 Evaluation of shear force tests

To aid simple slab design using Cobiax void formers it is useful to apply a constant factor $f_{Cobiax,\,EL}$ (EL for Eco-Line) as an input value for Equation 70 of DIN 1045-1. The factor describes the difference in shear resistance between the void former slab and a solid slab. The prefactor was determined in [6], among others. The test evaluation used below to derive $f_{Cobiax,\,EL}$ was based on Equation 70 of DIN 1045-1 [1] and Heft 525 of the Deutsche Ausschuss für Stahlbeton (German Committee for Reinforced Concrete) [7]. According to DIN 1045-1, Section 10.3.3, the design value of the shear resistance $V_{Rd,\,ct}$ for structural elements with bending reinforcement and without normal force and the necessary calculated shear reinforcement for normal-weight concrete is determined using the following equation:

$$V_{Rd,ct} = \frac{0.15}{\gamma_c} \cdot \kappa \cdot (100 \cdot \rho_l \cdot f_{ck})^{1/3} \cdot b_w \cdot d \qquad (1)$$

where: $\gamma_c = 1.50$ Partial factor for concrete

$\kappa = 1 + \sqrt{\frac{200}{d}}$ Scale factor

Table 1. Evaluation of Darmstadt tests on uniaxially stressed slabs

Specimen	h	d	b	A_{sl}	ρ_l	Mean $f_{cm,cube}$	Mean $f_{cm,cyl}$	κ	$V_{Rm,ct}$	Shear force V_E at failure in experiment (incl. loading device and dead weight)	$f_{Cobiax,EL}$
	mm	mm	mm	cm²/m	%	MN/m²	MN/m²	[–]	kN	kN	[–]
V1Da	300	260	820	19.4	0.75	22.70	18.2	1.9	191.0	107.6	0.56
V2Da	300	260	820	19.4	0.75	38.40	31.0	1.9	228.0	150.7	0.66
V3Da	300	260	820	19.4	0.75	49.50	40.1	1.9	248.5	143.9	0.58
V4Da	600	560	1550	35.4	0.63	17.80	14.3	1.6	577.1	362.0	0.63
V5Da	600	560	1550	35.4	0.63	51.00	41.3	1.6	823.0	424.8	0.52
V6Da	600	560	1550	35.4	0.63	65.50	53.4	1.6	896.2	431.5	0.48

Table 2. Evaluation of Kaiserslautern tests on slabs with oppositely acting moments

Specimen	Type	h	d	b	A_{sl}	ρ_l	Mean $f_{cm,cube}$	Mean $f_{cm,cyl}$	κ	$V_{Rm,ct}$	Shear force V_E at failure in experiment (incl. loading device and dead weight)	$f_{Cobiax,EL}$ and $V_E/V_{Rm,ct}$
		mm	mm	mm	cm²/m	%	MN/m²	MN/m²	[–]	kN	kN	[–]
V1KL-2009	Without void formers, with transversal bending	300	260	1420	18.7	0.72	61.72	50.2	1.9	458.2	414.8	0.91
V2KL-2009	With void formers, with transversal bending	300	260	1420	18.7	0.72	65.77	53.6	1.9	468.2	273.2	0.58
V3KL-2009	Without void formers, without transversal bending	300	260	1420	18.7	0.72	65.91	53.7	1.9	468.6	425.9	0.91

$$\rho_l = \frac{A_{sl}}{b_w \cdot d} \leq 0.02$$ Longitudinal rebar percentage

f_{ck} Characteristic value of concrete compressive strength in [N/mm²]
b_w Smallest cross-section width within the cross section tensile zone [mm]
d Effective structural height in [mm]

According to Figure H10-4 in Heft 525 [7] the mean shear resistance for slab-like structural elements without normal force can be determined as follows:

$$v_{Rm,ct} = 0.2 \cdot \kappa \cdot (100 \cdot \rho_l \cdot f_{c,test})^{1/3} \cdot b_w \cdot d \quad (2)$$

The prefactor 0.2 in the above equation describes the mean shear resistance in tests as compared to the design value according to Equation (1). The characteristic value of the prefactor for the corresponding equation is 0.14. The strength $f_{c,test}$ in the shear force test corresponds to the mean strength f_{cm} of the material specimen.

The Darmstadt tests V1Da to V6Da described in Section 2.1 are evaluated in Tables 1 and 2. The Cobiax factor $f_{Cobiax,EL}$, which describes the difference between the shear resistance of the Cobiax voided flat slab and the solid slab, is determined using Equation (3).

$$v_{Rct,Cobiax} = f_{Cobiax,EL} \cdot v_{Rct,DIN\ 1045\text{-}1}$$
$$= f_{Cobiax,\,EL} \cdot 0.2 \cdot \kappa \cdot (100 \cdot \rho_l \cdot f_{c,test})^{1/3} \cdot b_w \cdot d \quad (3)$$

where: b_w = overall width of slab.

The cylinder compressive strength $f_{c,test}$ from the 150 mm cube compressive strengths is calculated in Equation (3) as follows:

$$f_{c,cyl} = (0.7953 + 0.0003 \cdot f_{c,cube150}) \cdot f_{c,cube150} \quad (4)$$

The above equation describes a linear trend describing the conversion between cylinder/cube compressive strength to DIN 1045-1, Table 9. It covers strength types C12/15 to C55/67.

The tests carried out in Darmstadt and Kaiserslautern on Cobiax slabs without reinforcement cages have shown that adopting $f_{Cobiax,EL}$ as a reduction factor for Equation (3) for considering the reduced shear resistance resulting from the use of void formers leads to safe design values.

In the meantime the German Institute for Construction Technology has issued a technical approval for the system in which this reduction factor is employed [8]. It also regulates application boundaries, bending design rules and quality assurance measures during on-site execution.

3 Tests to determine the shear resistance on one-way spanning slabs with reinforcement cages

Ten slab strips fitted with the reinforcement cages indispensible to the Cobiax slab system (Figures 6 and 7) were also investigated at the Technical University of Kaiserslautern [9]. In the specimens shown here the resistance-welded reinforcement cages were installed in the stress axis (Figure 7). Depending on the void former diameter the stirrup arms cover a total area of 7.03 cm²/m² (void

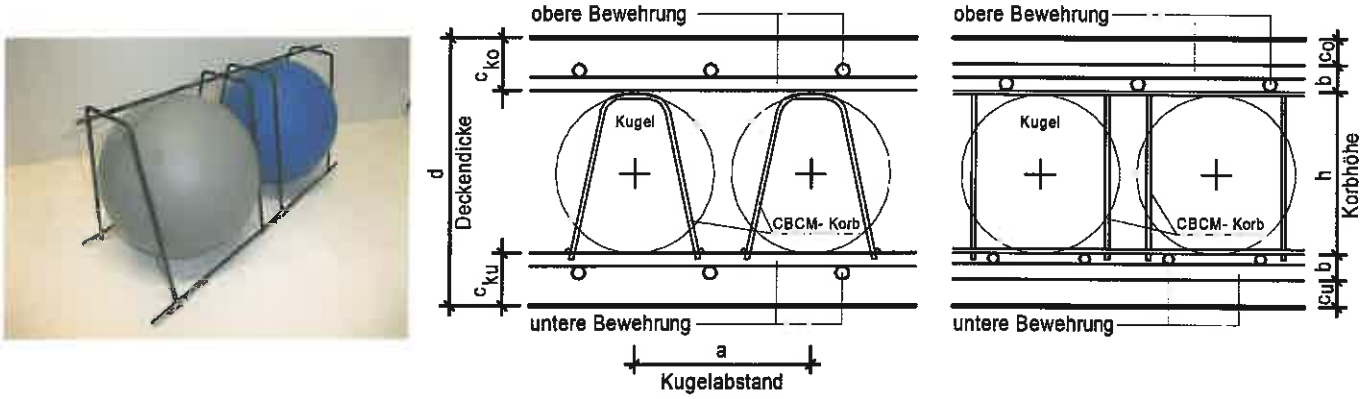

Fig. 6. Cobiax cage module detail, cross-section and longitudinal section of a multiaxially stressed cast-in-place Cobiax floor

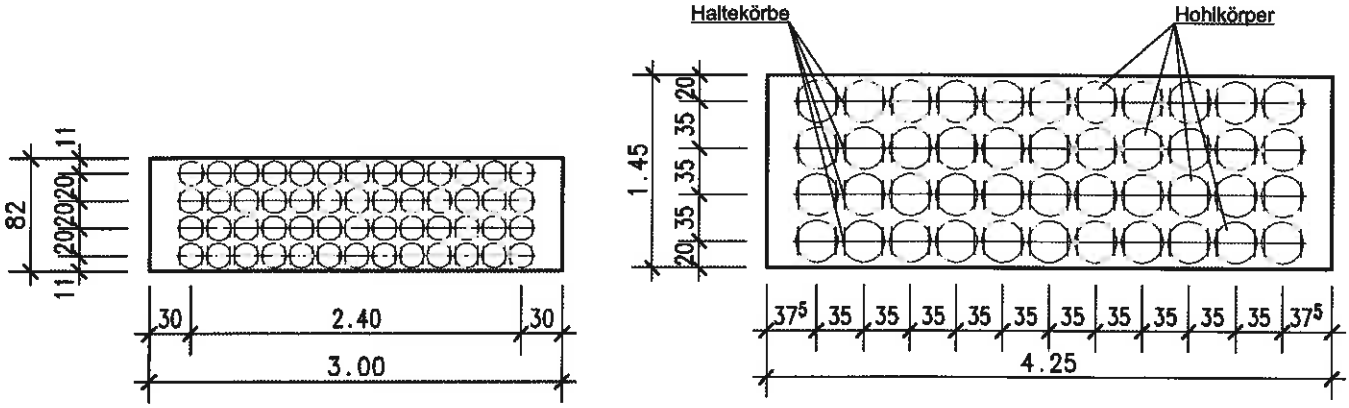

Fig. 7. Specimen ground plans of the first (left) and second (right) test series with marked cage modules

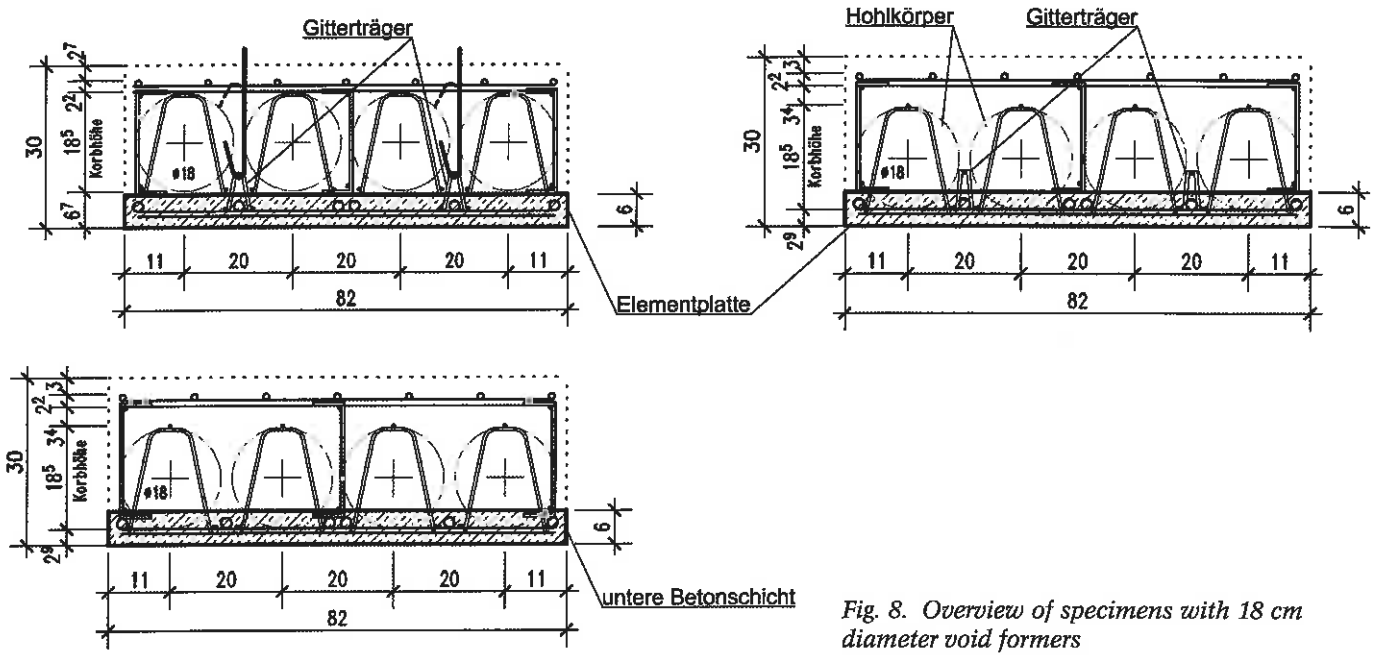

Fig. 8. Overview of specimens with 18 cm diameter void formers

Table 3. Evaluation of Kaiserslautern tests on uniaxially stressed slabs with reinforcement cages

	Test specimen	Execution method	h	d	b	A_{sl}	ρ_l	Mean $f_{cm,cube}$ Mean $f_{cm,cyl}$				κ	$V_{Rm,ct}$	Shear force V_E at failure in experiment (incl. loading device and dead weight)	$f_{Cobiax,EL}$ and $V_E/V_{Rm,ct}$
								Semi-precast slab	In-situ concrete	Semi-precast slab	In-situ concrete				
			mm	mm	mm	cm²/m	%	MN/m²	MN/m²	MN/m²	MN/m²	[–]	[kN]	[kN]	[–]
Series 1 (void former diameter 18 cm)	V1KL-2007	With cage module, on semi pre-cast slab	300	264	820	19.0	0.72	39.3	54.70	31.7	44.4	1.9	257.0	241.5	0.94
	V2KL-2007	With cage module, in semi pre-cast slab	300	264	820	19.0	0.72	39.3	54.70	31.7	44.4	1.9	257.0	312.6	1.22
	V3KL-2007	With cage module, without semi pre-cast slab	300	264	820	19.0	0.72	35.1	51.80	28.3	42.0	1.9	252.3	285.9	1.13
	V4KL-2007	Without cage module, without semi pre-cast slab	300	264	820	17.1	0.65	–	36.50	–	29.4	1.9	216.3	277.5	1.28
	V5KL-2007	Without cage module, with semi pre-cast slab	300	264	820	17.1	0.65	39.3	54.70	31.7	44.4	1.9	248.1	303.7	1.22
Series 2 (void former diameter 31.5 cm)	V6KL-2007	With cage module, on semi pre-cast slab	450	405	1450	21.9	0.54	38.6	45.20	31.1	36.6	1.7	540.5	635.4	1.18
	V7KL-2007	With cage module, in semi pre-cast slab	450	405	1450	21.9	0.54	38.6	45.20	31.1	36.6	1.7	540.5	619.6	1.15
	V8KL-2007	With cage module, without semi pre-cast slab	450	405	1450	21.9	0.54	38.6	44.80	31.1	36.2	1.7	538.9	584.3	1.08
	V9KL-2007	Without cage module, without semi pre-cast slab	450	405	1450	20.8	0.51	–	44.80	–	36.2	1.7	529.6	533.2	1.01
	V10KL-2007	Without cage module, with semi pre-cast slab	450	405	1450	20.8	0.51	38.6	45.20	31.1	36.6	1.7	531.2	626.9	1.18

former diameter 31.5 cm) to 21.6 cm^2/m^2 (void former diameter 18 cm). This corresponds to a geometrical rebar percentage ρ_{sw} of 0.07 % (void former diameter 31.5 cm) to 0.22 % (void former diameter 18 cm). The positioning cages and spacers provide shear reinforcement, the anchoring of which does not correspond to the requirements specified in DIN 1045-1, but which nevertheless affects the shear resistance.

Three different methods were used to manufacture the specimens in order to model the installation situations occurring in practice (Figure 8):

a. Precast element with positioning cages subsequently installed on the semi pre-cast slab.
b. Precast element with positioning cages encased in the concrete of the semi pre-cast slab.
c. In-situ concrete element concreted in two stages, with positioning cages encased in the lower section.

The difference in the procedure between b. and c. consisted of the lattice girders typical for prefabricated elements being integrated in the semi pre-cast slab for variant b., which was not the case for variant c.

In order to facilitate a direct comparison of the three Cobiax slabs with solid slabs a reference slab was manufactured for both series' (void former diameter 18 cm and 31.5 cm), respectively without void formers as a precast element with filigree slab and without void formers as a monolithic in-situ concrete element (see Table 3). A rebar percentage $\rho_1 = 0.51\%$ to 0.72 % was selected for the longitudinal rebars. The concrete strengths were determined on cubes of 150 mm side length and were between 35.1 and 54.7 N/mm^2. The net critical concrete cross-section perpendicular to the slab plane reduced by the void formers was 59 % and 52 % minimum respectively for the specimens with void former diameters 18 cm and 31.5 cm. The requirement in the permit [8] in terms of a minimum net concrete cross-section of 48 % was thus adhered to.

The tests were implemented as four-point bending tests. The shear slenderness was:

- a/d = 2.84 for five tests with void former diameter 18 cm.
- a/d = 2.72 for five tests with void former diameter 31.5 cm.

Inclined shear cracks appeared with increasing load, leading to a constriction of the compression zone. The specimens generally suffered shear-bending failure as a consequence of the increasingly small compression zone (cf. Figure 12).

As anticipated, it was shown that the rebar cages considerably increase the shear resistance, despite their anchoring in both the tensile and the compression zones not complying with DIN 1045-1.

The shear resistances achieved in the tests are summarised in Table 3. The shear resistance was determined at distance d from the support, taking the dead weight of the specimen into consideration. To calculate the shear resistance in Equation (2) $f_{cm,cyl}$ was adopted as $f_{c,test}$ for the in-situ concrete. The concrete of the semi pre-cast slabs always displayed lower compressive strength than the cast in-place concrete. However, it can be recognised from the failure crack patterns visible in Figure 12 that the strength of the semi pre-cast slabs, which were one fifth the thickness of the overall slab thickness at most, had barely any impact on the shear resistance.

A comparison of the shear resistances reveals that the specimens with positioning cages achieved at least 90 % of the theoretical shear resistance of a solid slab. The theoretical shear resistance was actually achieved or even exceeded in Series 2 (h = 45 cm). This indicates that the impact of the void formers on the shear resistance is compensated by the positioning cages acting as additional shear reinforcement. Using the current design concept the positioning cages are not adopted numerically to increase the shear resistance and thus generate a considerable reserve capacity.

4 Large-scale tests of multi-axial load-bearing capacity

In July 2009 the multi-axial load-bearing capacity was examined in a large-scale test at TU Kaiserslautern [10].

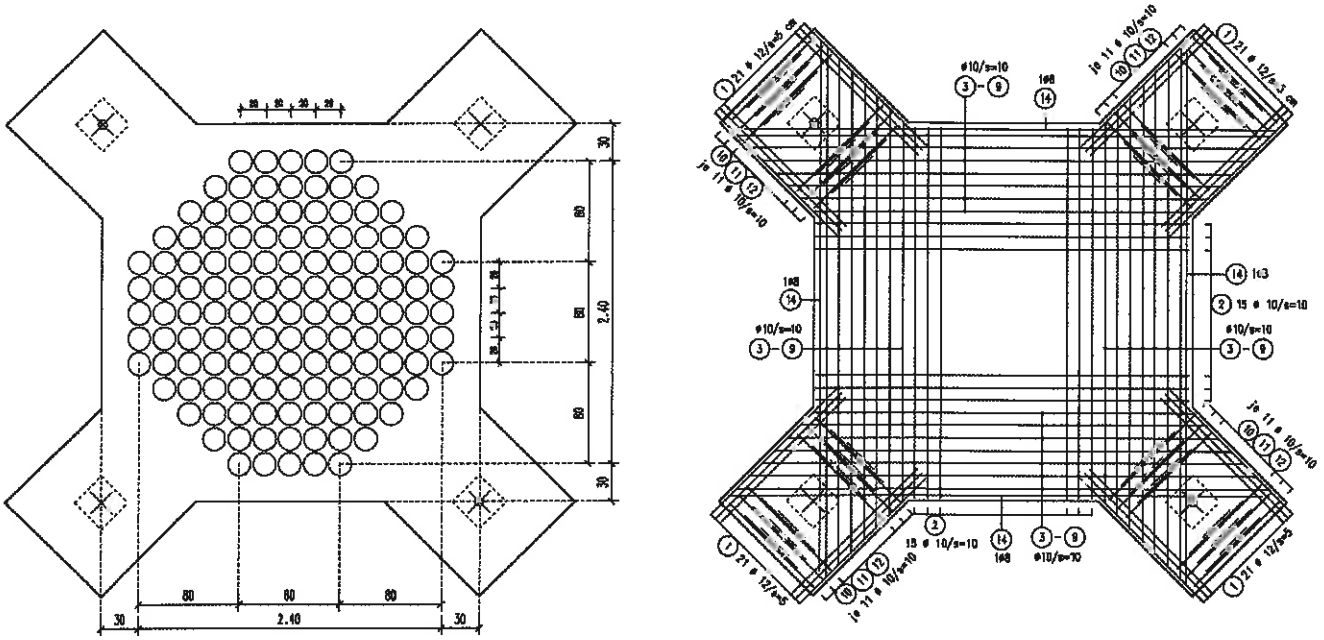

Fig. 9. Void former and reinforcement configuration in the tested specimen

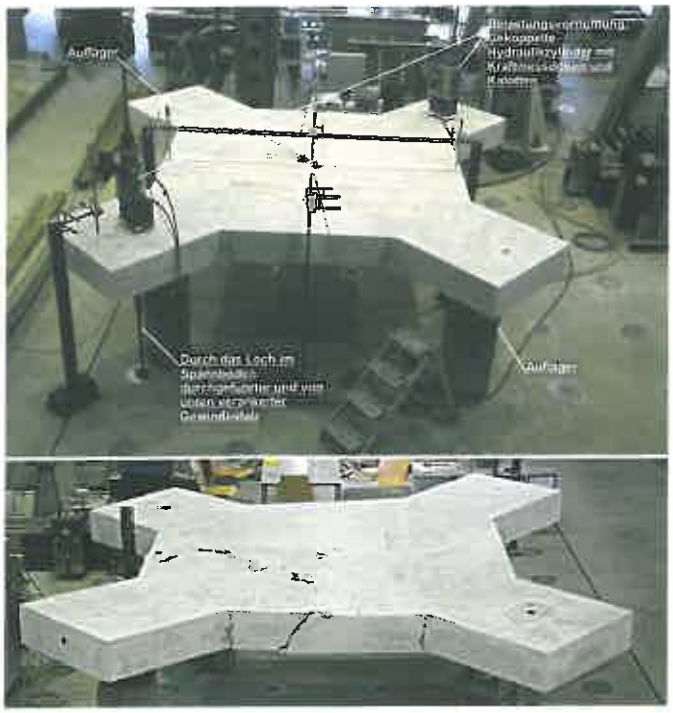

Fig. 10. Slab specimen in the test stand and failure pattern

The impact of torsion in a multi-axially stressed slab with Cobiax void formers was examined in this test. The reinforcement was arranged such that the direction of the principal reinforcement was not the same as the direction of the governing principal moments. The void formers were arranged on the same alignment as the reinforcement (Figure 9). The void formers in turn were held in position without the use of the usually installed positioning cages, in order to exclude their action as shear reinforcement. The slabs were h = 30 cm thick and the void former diameter d = 18 cm. The mean concrete compressive strength was 45.3 N/mm² (150 mm cube). Four brackets were attached to the slab. Two brackets were used for support, while a downward vertical load was applied on the other two (Figure 10) to generate a torsional load.

The crack pattern anticipated for torsional loading was produced during the test. Flexural bending cracks formed between the two load transfer points on the top and – rotated by 90° – between the two support points on the bottom. Failure occurred as a result of combined bending-shear failure in the end region of the bracket reinforcement (Figure 10). An impact of the void formers on the crack pattern produced could not be observed. This was confirmed by accompanying finite-element analyses. In order to allow comparison the slab was modelled both with and without void formers for the purpose of analysis. The previously computed failure load was achieved in the test.

The shear force achieved in the test is shown in Table 4. The actual width of the failure crack was adopted as the cross sectional width b. The shear force in the failure crack was also adopted as the shear force V_E achieved in the test and the dead load impact taken into consideration correspondingly. The impact of the longitudinal rebars on the shear resistance was considered as follows:

1. Only one layer of the lower longitudinal rebars was taken into consideration.
2. The resulting cross-section data of two successive rebar layers were incorporated as follows (also see [11]):

$$A_{sl} = \sqrt{A_{slx}^2 + A_{sly}^2} \tag{5}$$

5 Accompanying finite-element method analyses

To accompany the tests, physical, non-linear FEM analyses were carried out at the Institut für Beton- und Fertigteilbau at Bochum University [11]. The DIANA [12] program was used for this. The good suitability of this program for realistic numerical simulations of concrete structural elements has already been shown in [3] and [4]. 20-node quadratic isoparametric elements were employed in the model. The FEM mesh used to model the slab geometry with void formers is reproduced in Figure 11.

The *Thorenfeldt* [13] model was employed as the constitutive equation for the concrete in the compression zone. The *Hordijk* model was used for the tensile zone [12], [14]. The fracture energy governing the falling arm of the stress-strain relationship is incorporated in DIANA with the aid of Model Code 90 [15]. Cracks running parallel to the compressive stress axis impact the compressive strength of the concrete. This effect was taken into consideration with the aid of the *Vecchio* And *Collins* approach by reducing the uniaxial compressive strength by a factor β as a function of the transverse tensile strain [15]. The impact of any constrained transverse dilatation on compressive strength is described using the *Selby* And *Vecchio* approach [17].

A bilinear stress-strain curve without hardening and – with an eye on reasonable computing time – a model with "smeared" reinforcement were selected. This

Table 4. Evaluation of torsion test

Evaluation of longitudinal rebars	h	d	b	A_{sl}	ρ_l	Mean $f_{cm\cdot cube}$	Mean $f_{cm\cdot cyl}$	κ	$V_{Rm\cdot ct}$	Shear force V_E at failure in experiment (incl. loading device and dead weight)	$f_{Cobiax\cdot EL}$
	cm	cm	cm	cm²	%	MN/m²	MN/m²	[–]	kN	kN	[–]
One rebar layer	30	27	175	9.714	0.21	45.29	36.6	1.86	344.7	200.2	0.58
To [11]	30	27	175	13.74	0.29	45.29	36.6	1.86	386.9	200.2	0.52

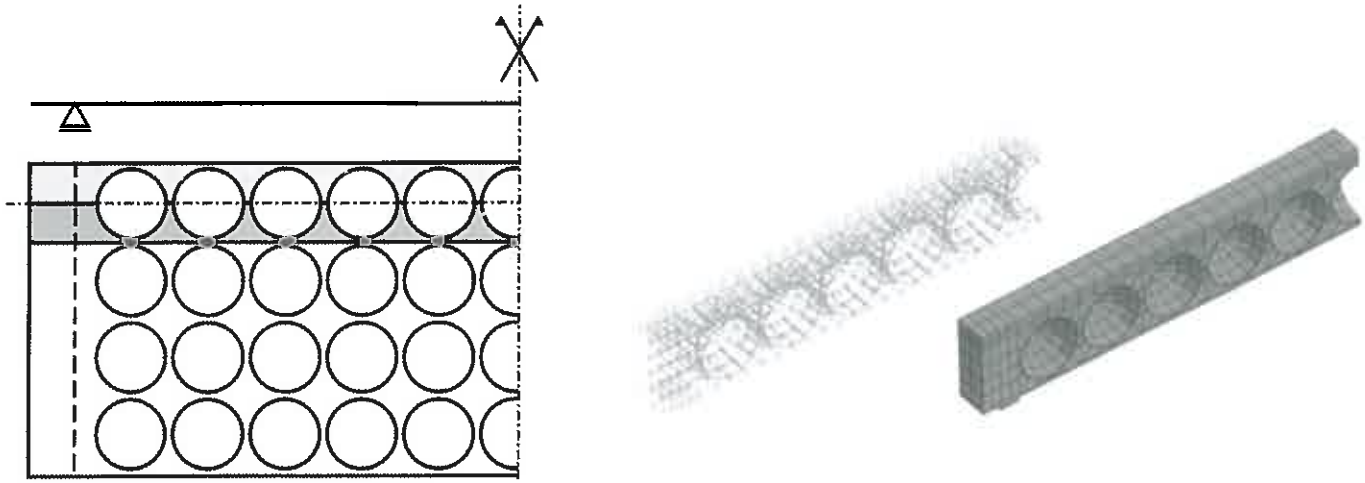

Fig. 11. 1/16 slab strips utilising symmetry conditions and finite element model

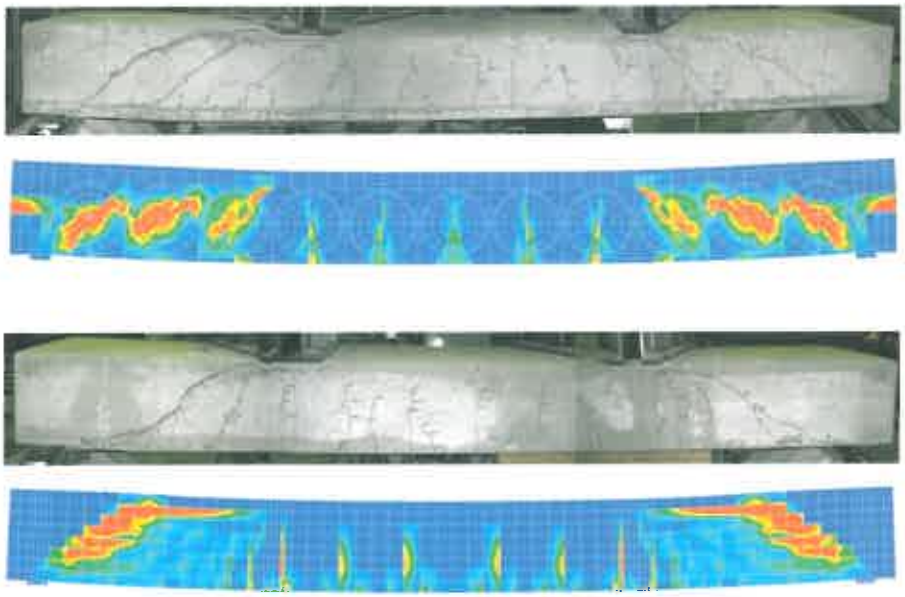

Fig. 12. Crack patterns and principal strains of specimens, a) with void formers (V8KL-2007) and b) without void formers (V9KL-2007)

increases the stiffness of the elements penetrated by the reinforcement as a function of the rebar percentage.

Analysis using "smeared" cracking followed. If crack formation occurs as a result of exceeding the tensile strength, the tangential and normal stiffnesses are reduced. The element with originally isotropic material behaviour now has different stiffnesses in each direction. The *Hordijk* model discussed above is employed to take tension softening normal to the direction of crack orientation into consideration. Tangentially, the shear modulus was reduced using the shear retention factor to model the cracking friction. To model the scale effect the β-values are varied between 0.02 (h = 45 cm) and 0.07 (h = 20 cm) proportional to the slab thickness. The β-values employed are thus in the usual range between 0.01 and 0.1 [18].

Realistic modelling of crack propagation is critical for numerical simulation of the shear load-bearing behaviour. In the cases of shear-bending failure and shear-tension failure observed in the tests in particular, crack propagation in the compression zone leads to weakening of the concrete resistance share and finally to failure. The positioning cages used in the tests described in Section 3 were therefore also taken into consideration in modelling. However, while tests using void formers without positioning cages provided a good correlation with FEM analysis results in earlier investigations [4], these were the first FEM analyses using positioning cages in simulation.

Figure 12 shows the crack patterns observed in the tests described in Section 3 with positioning cages installed for both a solid slab (V9KL-2007) and a void former slab (V8KL-2007), as well as the principal tensile strains in the ultimate limit state in the corresponding FEM analyses. Comparing the crack patterns to the principal strains shows that the FEM model used realistically models the cracking behaviour of the investigated specimens both with and without void formers.

Figure 13 also shows a comparison of the force-deformation relationships between the tests and the FEM analyses. It is apparent that the force-deformation relationships in the FEM model correlate well with the behaviour of the specimen in terms of both the stiffness and the failure loads.

The two diagrams also include the calculated shear resistance to aid assessment of the results. The concrete resistance share $V_{Rm,ct}$ without shear reinforcement is determined compliant with DIN 1045-1, Eq. 70 using the

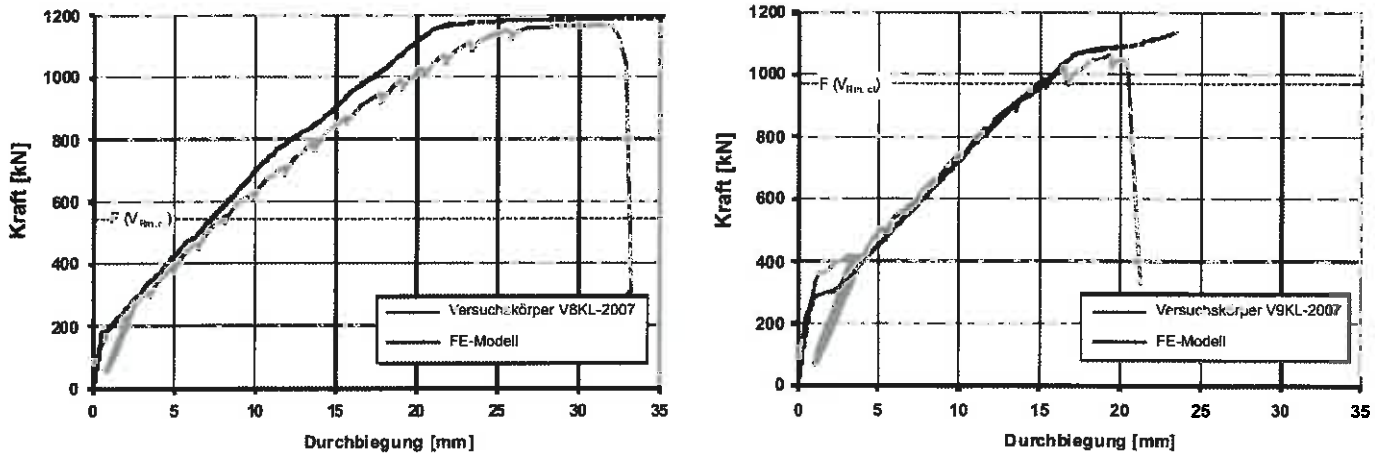

Fig. 13. Force-displacement relationships of a specimen with void formers and without (h = 45 cm)

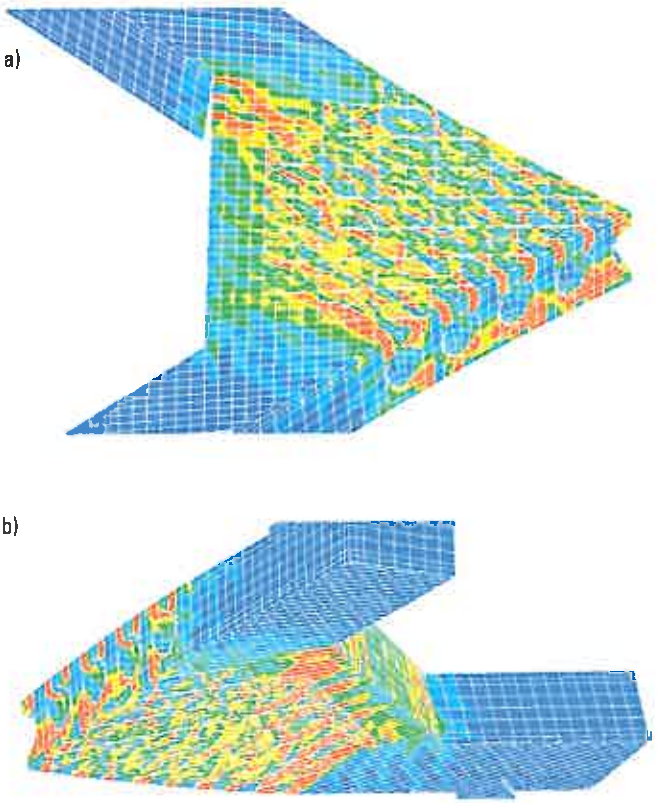

Fig. 14. Crack patterns (principal strains) obtained from the finite element analysis, a) top and b) bottom

prefactor 0.2. For comparison $V_{Rm,ct}$ is reduced by 50% to take weakening by the void formers into consideration. Here, too, it is obvious that the bearing capacity of the void former slabs is considerably increased by the positioning cages.

It is obvious that the action of the cages and spacers as shear reinforcement is realistically represented in the FEM model. In the specimens using void formers this achieves a shear resistance more than double the calculated concrete resistance share $V_{Rm,ct}$.

In order to examine the relevance of the FEM model as applied to a bi-axial load transfer a comparative analysis was also carried out for the large-scale test described in Section 4. Utilising system symmetry a quarter of the test slab was analysed in the FEM model.

The cracking pattern produced in the FEM analysis corresponded to that anticipated for torsion (Figure 14). Flexural bending cracks, running perpendicular to a line connecting the two load transfer points, formed on the upper face. The crack orientation on the lower face was rotated by 90° and therefore perpendicular to a line connecting the two support points.

The cracking patterns identified using FEM analyses display good correlation with the cracking patterns observed in the test.

The FEM analyses reproduced here as examples prove the fundamental suitability of the software used. The necessary input parameters for the non-linear analyses were calibrated in comprehensive preliminary studies. Additional analyses are planned using the selected models and altered void former installation configurations in section and in plan.

6 Summary

A design concept for the shear resistance of reinforced concrete slabs with spherical void formers corresponding to a previously issued technical approval [8] was derived from the test results. It also regulates application boundaries, bending design rules and quality assurance measures during on-site execution. In this approval the reduction factor for calculating the shear resistance was defined as $f_{Cobiax,EL} = 0.50$.

Figure 15 compares the results gained in the test with the results for solid slabs. The prefactor values used there were computed for Cobiax tests as follows:

$$\text{Prefactor} = \frac{V_E}{\kappa \cdot (100 \cdot \rho_l \cdot f_{c,test})^{1/3} \cdot b_w \cdot d} \cdot \frac{1}{f_{Cobiax,EL}} \qquad (6)$$

where: V_E = shear force at failure in the respective experiment.

The Cobiax values are considerably greater than the mean values for solid slabs and all are far greater than the 5% fractile. In practice, the positioning cages represent a considerable, unutilised reserve in load-bearing capacity.

Tests with multiaxial loading were carried out in addition to pure shear force tests. In these tests it was possible

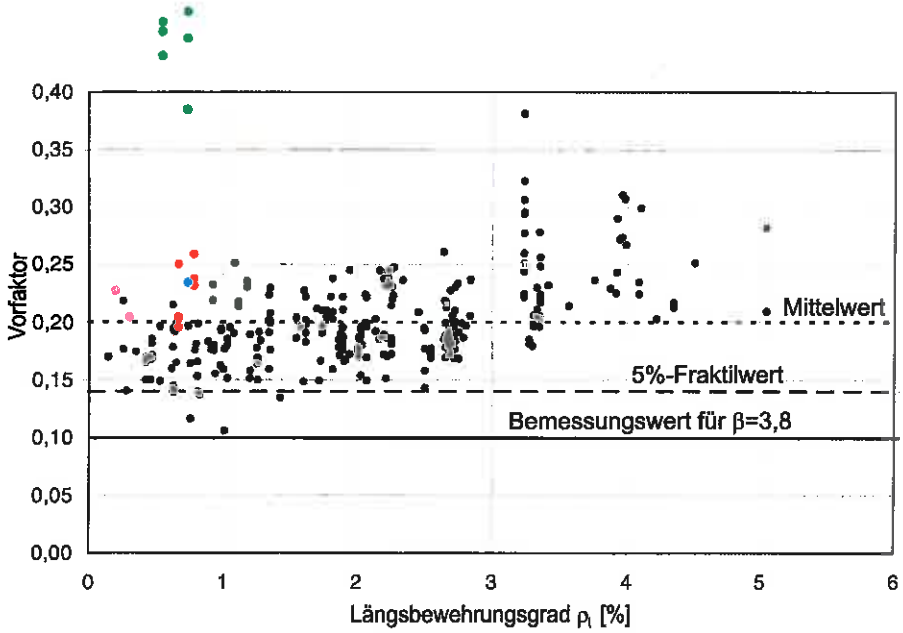

Fig. 15. Empirical identification of the coefficient for Equation (70) of DIN 1045-1 from [7] and shear force capacities obtained in the tests on the Cobiax system

to confirm the multiaxial action of reinforced concrete slabs with spherical void formers.

7 Outlook

An initial test series was carried out on ten specimens at the Institut für Beton- und Fertigteilbau at Bochum University using a new, flattened void former shape (Figure 16) [19], [20]. A variety of void former configurations were used (with and without positioning cages, in-situ concrete and precast element solution, parallel and diagonal orientation, normal spacing and tightly spaced). As anticipated, the shear force achieved during the tests in the slabs with void formers was in a range between 49% and 66% of that for the investigated solid slabs. Based on this initial test series the load-bearing behaviour of reinforced concrete slabs employing these innovative void formers will be investigated in more detail in future research projects.

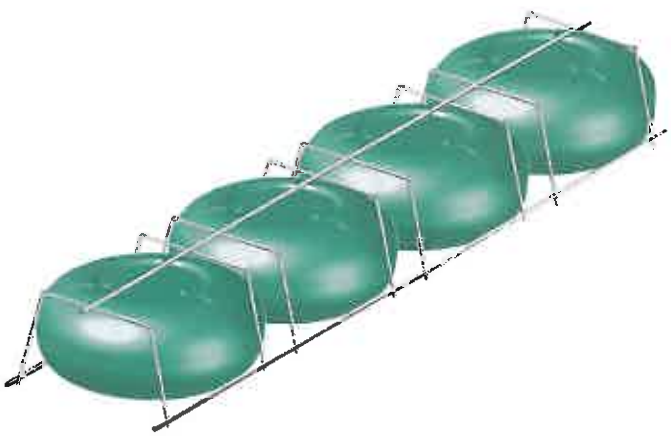

Fig. 16. Cage module with flattened void formers

References:

[1] DIN 1045-1: Concrete, reinforced and prestressed concrete structures – Part 1: Design and construction. August 2008

[2] *Schnellenbach-Held, M., Pfeffer, K.*: Tragverhalten zweiachsiger Hohlkörperdecken. Beton- und Stahlbetonbau 96 (2001) Heft 9, pg. 573–578, 2001

[3] *Pfeffer, K.*: Untersuchungen zum Biege- und Durchstanztragverhalten von zweiachsigen Hohlkörperdecken, Dissertation. Fortschritt-Bericht VDI Reihe 4 Nr. 178, Düsseldorf, 2002

[4] *Aldejohann, M.*: Zum Querkrafttragverhalten zweiachsiger Hohlkörperdecken, Dissertation. Universität Duisburg-Essen, Fachbereich Bauwissenschaften 2009

[5] *Schmidt, H*: Untersuchungsbericht Nr. 091.01.08: Querkrafttragfähigkeit von Cobiax-Hohlkörperdecken ohne Fixierungskörbe. Technische Universität Darmstadt, 5. September 2008

[6] *Hegger, J., Roeser, W.*: Gutachten zur Querkrafttragfähigkeit von Stahlbetondecken mit Cobiax-Hohlkörpern. Hegger + Partner, Aachen, 2008

[7] Erläuterungen zu DIN 1045-1. Heft 525 des Deutschen Ausschusses für Stahlbeton, Entwurf der 2. Auflage. Beuth Verlag GmbH, Berlin, 2010

[8] Allgemeine bauaufsichtliche Zulassung Z-15.1-282: Hohlkörperdecke System „Cobiax". Deutsches Institut für Bautechnik, Berlin, 5. Februar 2010

[9] *Schnell, J.*: Versuchsbericht 07045Ab/512: Querkraftversuche an Hohlkörperdecken. Technische Universität Kaiserslautern, 10. Januar 2008

[10] *Schnell, J.*: Versuchsbericht 09040Ab/538: Drillversuch an einer Hohlkörperdecke. Technische Universität Kaiserslautern, 1. September 2009

[11] *Albert, A., Nitsch, A.*: Gutachten zum Tragverhalten und zur Bemessung von Decken mit Hohlkörperelementen der Fa. Cobiax Technologies. Institut für Betonfertigteilbau, Bochum, 2009

[12] DIANA User's Manual Release 9, TNO, 2005

[13] *Thorenfeldt, E.; Tomaszewicz, A.; Jensen, J. J.*: Mechanical properties of high-strength concrete and applications in de-

sign. In Proc. Symp. Utilization of High-Strength Concrete (Stavanger, Norway), Ed. Trondheim, Tapir, 1987
[14] *Hordijk, D. A.*: Tensile and fatigue behaviour of concrete, experiments, modeling and analyses. Heron, Vol. 37, No. 1, Delft, 1992
[15] CEB-FIP MODEL CODE 1990 Design Code, Comite-Euro-International du Beton, 1991
[16] *Vecchio, F.J.; Collins, M.P.*: The modified compression field theory for reinforced concrete elements subjected to shear. ACI Journal 83, 22 1986
[17] *Selby, R.G.; Vecchio, F. J.*: Three-dimensional constitutive relations for reinforced concrete, Tech. Rep. 93-02, Univ. Toronto, Dep. Civil Engineering, Toronto, Canada, 1993
[18] *Kolmar, W.*: Beschreibung der Kraftübertragung über Risse in nichtlinearen Finite-Element-Berechnungen von Stahlbetontragwerken, Dissertation TH Darmstadt, 1986
[19] *Albert, A., Nitsch, A.*: Bericht zu Querkraftversuchen an Hohlkörperdecken. Hochschule Bochum, 15. Februar 2008
[20] *Eilers, S.*: Querkrafttragfähigkeit von Hohlkörperdecken, Masterthesis, Hochschule Bochum, 2008

Dr.-Ing. Marcin Abramski
Technische Universität Kaiserslautern
Fachgebiet Massivbau und
Baukonstruktionen
67653 Kaiserslautern
mabramski@rhrk.uni-kl.de

Prof. Dr.-Ing. Andrej Albert
IfBF – Institut für Beton- und
Fertigteilbau GmbH & Co. KG
An-Institut der Hochschule Bochum
Lennershofstraße 140
44801 Bochum
albert@ifb-fertigteilbau.de

Dr.-Ing. Karsten Pfeffer
Cobiax Technologies GmbH
Heidelberger Straße 6-8
64283 Darmstadt
karsten.pfeffer@cobiax.com

Prof. Dr.-Ing. Jürgen Schnell
Technische Universität Kaiserslautern
Fachgebiet Massivbau und
Baukonstruktionen
67653 Kaiserslautern
jschnell@rhrk.uni-kl.de